



Predicting pavement performance using distress deterioration curves

Ahmed Abed, Mujib Rahman, Nick Thom, David Hargreaves, Linglin Li & Gordon Airey

To cite this article: Ahmed Abed, Mujib Rahman, Nick Thom, David Hargreaves, Linglin Li & Gordon Airey (2024) Predicting pavement performance using distress deterioration curves, Road Materials and Pavement Design, 25:6, 1174-1190, DOI: [10.1080/14680629.2023.2238094](https://doi.org/10.1080/14680629.2023.2238094)

To link to this article: <https://doi.org/10.1080/14680629.2023.2238094>



© 2023 The Author(s). Published by Informa UK Limited, trading as Taylor & Francis Group



Published online: 13 Sep 2023.



Submit your article to this journal [↗](#)



Article views: 1168



View related articles [↗](#)



View Crossmark data [↗](#)



Citing articles: 1 View citing articles [↗](#)

Predicting pavement performance using distress deterioration curves

Ahmed Abed ^a, Mujib Rahman^a, Nick Thom^b, David Hargreaves^b, Linglin Li^b and Gordon Airey^b

^aDepartment of Civil Engineering, Aston University, Birmingham, UK; ^bFaculty of Engineering, University of Nottingham, Nottingham, UK

ABSTRACT

Highway Authorities in the UK use Surface Condition Assessment for the National Network of Roads (SCANNER) in assessing and managing their road networks. This survey vehicle utilises laser measurements to detect and quantify most of the distress on the road surface, such as rutting, cracking and texture depth. It is however a data intensive and expensive approach since it is conducted annually. This study presents a simple method to predict pavement distress using previous SCANNER measurements. The previous measurements are used to develop Distress Deterioration Master Curves (DDMC) that relate distress deterioration rate with the severity of the distress. These curves can be used to predict future distress severity based on the current state without the need to provide further data such as pavement age or pavement material properties. To demonstrate the application of this method, a significant amount of SCANNER data covering around 400 km of class A roads in Nottinghamshire collected between 2014 and 2020 were analysed, and rutting, crack intensity, and texture depth were modelled in this study. DDMRs of these distress types were built based on data collected between 2014–2018, then 2020 data were used to validate the predictions. The results show that the developed method can be implemented in predicting surface distress of roads using previous measurements, which makes it a valuable addition tool for highway authorities subject to underfunding.

ARTICLE HISTORY


Received 16 December 2022
Accepted 13 July 2023

KEYWORDS

Pavement performance; distress prediction; modelling; deterioration curves

1. Introduction

Pavement structures exhibit different types of distress due to traffic loading and environmental conditions, such as rutting (Kim et al., 2000; Perraton et al., 2010; Wang et al., 2022), fatigue cracking (Di Benedetto et al., 2004; Luo et al., 2018; Mbarki et al., 2012), thermal cracking (Alavi et al., 2015; Dave & Buttlar, 2010; Epps, 2000), or surface texture deterioration (Mansura et al., 2018; Xiao et al., 2020). These distress types have multiple effects on road networks; they increase the pavement roughness (Můčka, 2016; Sandra & Sarkar, 2013), reduce road user comfort (Ahlin & Granlund, 2011; Guha & Hosain, 2022), increase vehicle fuel consumption (Perrotta et al., 2019; Svenson & Fjeld, 2015) which increases CO₂ emissions, raise the number of road user compensation claims (Asphalt Industry Alliance, 2022), and increase the risks of traffic accidents (Chan et al., 2010; Tamakloe et al., 2021). It is therefore of paramount importance to monitor pavement surface condition and assess the extent of the distress to minimise these effects and manage road networks efficiently.

CONTACT Ahmed Abed  abeda@aston.ac.uk

© 2023 The Author(s). Published by Informa UK Limited, trading as Taylor & Francis Group.

This is an Open Access article distributed under the terms of the Creative Commons Attribution License (<http://creativecommons.org/licenses/by/4.0/>), which permits unrestricted use, distribution, and reproduction in any medium, provided the original work is properly cited. The terms on which this article has been published allow the posting of the Accepted Manuscript in a repository by the author(s) or with their consent.

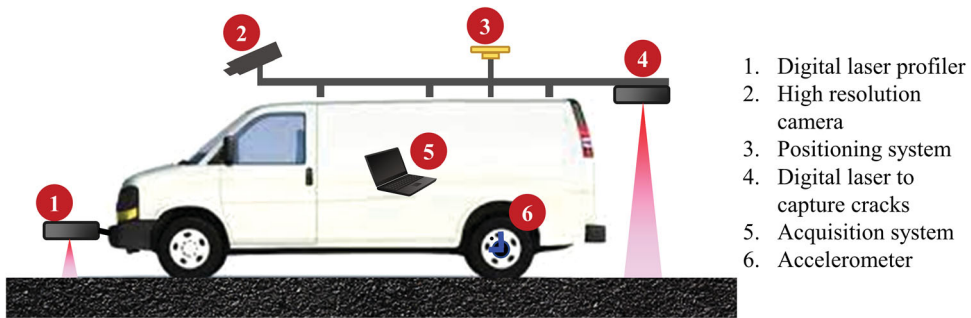
Different methods have been developed to monitor and assess the surface condition of roads. In general, these methods can be categorised into two types, manual visual surveys, and automated surveys. In the UK, two visual survey methods are frequently used, Coarse Visual Inspection (CVI) and Detailed Visual Inspection (DVI) (Department for Transport, 2021). These methods are mainly applied nowadays to assess the condition of the unclassified road networks in the UK, the difference being that a CVI can be performed from a slow-moving vehicle whereas a DVI is a walked survey but more comprehensive and detailed than the CVI. On the other hand, automated surveys rely on laser sensor measurements and road surface images to assess road condition. Two automated Traffic Speed Survey (TTS) methods are implemented in the UK, Traffic Speed Condition Surveys (TRACS), which is mostly used on the trunk road network, and SCANNER, which is used by local highway authorities to scan class A, B and C roads (Department for Transport, 2021; Mcrobbie et al., 2007); A roads are major roads designed to link major areas, B roads feed traffic onto A roads from adjacent areas, and C roads are smaller links between villages, towns, or other housing or industrial areas (Department for Transport, 2012).

Apart from these two survey methods, there are numerous studies in the literature on road survey methods and the key issues with each method such as the accuracy of the measurements, survey speed, repeatability and reproducibility of the results (Chu et al., 2022; Ragnoli et al., 2018; Shtayat et al., 2020). Since this study is concerned with modelling pavement performance using SCANNER then this survey method is given more attention. Figure 1 shows the main components of a typical SCANNER vehicle; it has: two digital laser sensors that are used to capture surface distress, transverse profile, longitudinal profile, and edge condition of roads (UK Roads Board, 2011b). Some SCANNER vehicles implement artificial intelligence and image processing technologies to better identify the cracks (PTS, 2022). Over 40 indicators are extracted from the laser measurements, these include rutting, cracking, longitudinal profile variance, texture depth, and edge condition; the other indicators are basically different forms of reporting these distress types (UK Roads Board, 2011a). Highway authorities process these data to calculate one indicator, namely Road Condition Index using the following equation:

$$\begin{aligned}
 RCI = & \max(R_{LW}, R_{RW}) \times RW_R \times IW_R + T \times RW_T \times IW_T \\
 & + CI \times RW_C \times IW_C \\
 & + \max(LPV_3 \times RW_{LPV_3} \times IW_{LPV_3}, LPV_{10} \times RW_{LPV_{10}} \times IW_{LPV_{10}})
 \end{aligned}$$

where R_{LW} , R_{RW} are rutting scores in the left and right wheel paths, T is the texture depth score, CI crack intensity score, LPV is the longitudinal profile variance score over 3 or 10 metres, RW and IW are reliability and importance weightings that depend on the class of the road and can be found in (UK Roads Board, 2011a). The RCI is calculated for every 10 metres of the surveyed roads and based on its value the condition of the sections is ranked into three levels: green for $RCI \leq 40$, orange for $40 < RCI \leq 100$, and red for $RCI > 100$; these ranks are used to manage the road network and plan maintenance activities.

On the other hand, various different methods have been developed to model pavement deterioration. Mechanistic models (Abu Al-Rub et al., 2012; Dinegdae & Birgisson, 2016) rely on methods such as fracture mechanics and constitutive modelling to predict pavement distress. Mechanistic-empirical models (ARA, 2004; Luo et al., 2017) combine the mechanistic response of pavement structures (i.e. stresses and strains) with empirical regression models to predict pavement performance. Empirical models use methods such as machine learning or statistical regression to predict pavement performance (Kargah-Ostadi & Stoffels, 2015; Marcelino et al., 2019; Yu et al., 2007). Further, due to the stochastic nature of pavement performance (Darter & Hudson, 1973), researchers have also developed probabilistic methods to model pavement deterioration, such as Monte Carlo simulation (Abed et al., 2019; Wang et al., 2010), and Markov Chains (Abaza, 2015; Alimoradi et al., 2020); Artificial Neural Networks have also been widely applied in predicting pavement performance (Wang et al., 2022; Zhou



1. Digital laser profiler
2. High resolution camera
3. Positioning system
4. Digital laser to capture cracks
5. Acquisition system
6. Accelerometer

Figure 1. A typical SCANNER system.

et al., 2021). Most of these methods however require various inputs such as material properties, pavement structural data, pavement age, climate data, or traffic data (Ziari et al., 2015), which may limit their implementation.

Highway authorities in the UK conduct annual road distress surveys to assess the condition of the road network, calculate RCI, and plan maintenance activities. This process however is expensive and time consuming, which exerts an additional economic burden on the already underfunded budget allocated for the maintenance of the roads. Therefore, the aim of this study is to develop a simple model capable of predicting the future condition of a pavement surface based on its current condition using a new approach called Distress Deterioration Rate (DDR). By this approach, the DDRs are calculated using previous SCANNER measurements depending on the severity of each distress, these are used to construct deterioration curves that can be used to predict the future level of the distress depending on its current level only. A similar approach has been suggested in literature to predict pavement deterioration rate expressed by a drop in Pavement Condition Index (PCI) by Kargah-Ostadi et al. (2019). In that study, the authors built a PCI deterioration curve in which the average drop in the PCI is dependent on the current PCI value. The PCI deterioration curve was built using the previous two measurements where the deterioration rate was calculated as the drop in the PCI divided by the time lag between the measurements. This study demonstrated that the PCI deterioration rate is low when the pavement condition is good ($PCI > 90$) and also when it is bad ($PCI < 40$). This is probably because the PCI score is scaled to be between 0–100 rather than because of a change in the deterioration rate of the distress types included in the PCI calculations. Accordingly, this method has been implemented in this study but with some modifications. Firstly, using two measurements to determine a deterioration rate may not be sufficient; the deterioration rate may vary considerably from one year to another, therefore obtaining the deterioration rate as an average of a longer period is more accurate. Secondly, the PCI is a function of various distress types, with each having a certain weight and reliability factors, and distress deterioration may increase, decrease, or remain constant over time. Accordingly, every distress should be modelled individually to exclude the effects of the other distress types, weighting and reliability factors on the Distress Deterioration Rate (DDR). Furthermore, based on the data collected in this study, we find that DDRs are functions of the current condition or deterioration level of the pavement. This means that a few deterioration models rather than one might be required to predict a distress type, where every model is required to fit certain distress severity data. Despite this approach being applicable, it is not practical as the number of models might be very high. To this end, we introduce in this study a novel method to construct a distress deterioration master curve from the individual DDR models. The distress deterioration master curve can then be used to predict the future level of the distress based on its current level. By implementing the suggested approach and the stated modifications, rutting, cracking, and texture depth have been selected to demonstrate the application of the suggested method. The results show that this approach has a reasonable accuracy and could be a valuable additional tool for highway authorities, allowing them to reduce their spending on pavement condition assessment.

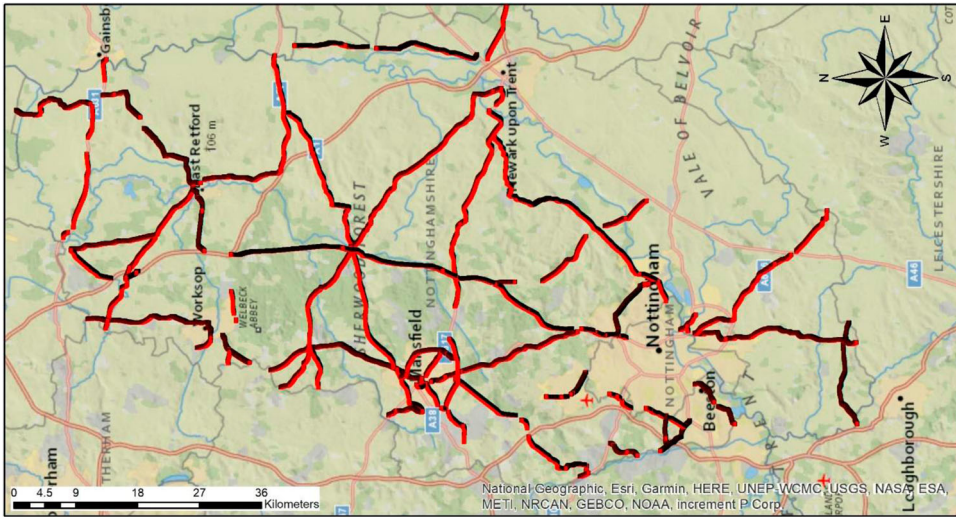


Figure 2. A map showing the study area and the road sections used in this study (The shown points represent the scanned road sections; bridges, roundabouts, and intersections were not included in the survey).

Table 1. Sample of the raw SCANNER data used in this study.

Section ID	Type	Start	End	Rutting in left wheel path mm	Rutting in right wheel path mm	Texture depth mm	Longitudinal profile variance over 3m m ²
3055A6005201	A	0	10	2.5	3	0.85	0
3055A6005201	A	10	20	2.9	5.8	0.19	0
3055A6005201	A	20	30	3.3	7.6	0.54	0.7

2. Materials and methods

2.1. Data description and pre-processing

In this study, a significant amount of SCANNER data from around 400 km of class A roads in Nottinghamshire were collected; Figure 2 presents a map showing a sample of these data. The data were supplied in a text file format as used in the UK Pavement Management System (UKPMS) software. The data are structured to report 44 data points that include distress measurements, different forms to express the distress, section geometries, and section coordinates of every 10 metres of the scanned network. The data cover the inner lane of one direction of the roads, which had been scanned every two years between 2014 and 2020, and they amount to about 40 thousand sections. A sample of the raw data is presented in Table 1.

These data however may contain inherent issues such as error in measurements, missing data, spatial variability, inaccurate section boundaries, or even outliers which may happen due to localised issues such as drainage problems (Kargah-Ostadi et al., 2019), or even updating data analysis algorithms or SCANNER laser sensors over time. Another issue with the data is maintenance and rehabilitation activities which are manifested as improvements in the pavement condition or a reduction in distress levels. These issues can lead to a large bias in the calculations of DDRs and should be treated before attempting to build deterioration models.

Many methods to reduce the effects of these issues on the quality of data have been suggested in literature (Kargah-Ostadi et al., 2019), as shown in Table 2. Every one of these methods is suited to a specific issue in the data. For instance, if a set of data is missing, then an averaging or interpolation process can be followed to estimate the missing data. Likewise, if a dataset is suspected to have a measurement error or maintenance was provided, then the outlier removal method can fix this situation.

Table 2. Data pre-processing methods (Kargah-Ostadi et al., 2019).

Data issue	Pre-processing technique
Spatial Variability	Dynamic Segmentation for Model Development; Probabilistic Model Development; Smaller Segments for Model Development
Inaccurate Section Boundaries	Controlling Standard Deviation in Segmentation
Temporal Variability	Combining Sections and Averaging
Noise	Smoothing / Moving Average; Benchmarking
Outliers (Unreasonable Data)	Smoothing / Moving Average
Missing Data	Outlier Removal
Scale Differences	Averaging / Interpolation; Bootstrapping; Imputation
Inter-Correlation of Input Data	Normalization
Measurement Errors/ Subjectivity	Principal Components Analysis; Stepwise Regression; Variable Multiplication
	Outlier Removal; Averaging; Benchmarking

In this study, two methods were followed to pre-process the data. Firstly, the sections that showed a reduction in distress level were filtered from the data using the outlier removal method. This is to exclude sections that might have received maintenance or might contain an error. Secondly, when joining sections from different years, some sections presented error at the boundaries. In other words, there was some distance difference in these sections from one year to another. This could be due to an error in identifying the start stations of roads, the temporal separation between the surveys which may affect sensor accuracy or analysis algorithm of sensor data, or survey staff change from one survey to another. To solve this issue, an outlier removal based on the distance was applied; basically, the sections that showed a difference in the distance of more than a threshold value of 5 m measured centre to centre, which is 50% of a section length, were excluded from the data; this is to assure that the same section is being monitored over time. Lastly, there was no concern about spatial variability in the data since the maximum section length was 10 m, and it is quite unlikely in this length that a significant change in pavement condition occurs. Following these techniques, the data was pre-processed and used in building deterioration models as explained in the following section.

2.2. DDR model development

Pavement distress increases over time due to traffic loading and environmental conditions such as ageing and thermal stresses. If the distress is surveyed repeatedly over a period of time, and in the absence of intrinsic pavement modelling inputs such as material properties and pavement design, then one can adopt a mathematical approach to model the rate of distress deterioration, as follows:

$$DDR_i = (D_i - D_{i-1}) / ((T_i - T_{i-1})) \quad (1)$$

where DDR is distress deterioration rate, D is the distress magnitude, i is the survey number, and T is the time of the survey. The data in this study however show that DDR is not linear; rather it is dependent on the magnitude or severity of the distress, or pavement structural condition in general (Abaza, 2014). Therefore, the previous equation can be rewritten as follows:

$$DDR_{i,s} = (D_{i,s} - D_{i-1,s}) / ((T_i - T_{i-1})) \quad (2)$$

where s is the severity of the distress in question. This equation can be used to calculate the DDR considering the current structural condition or the distress severity, which in turn can be used to predict the distress magnitude as follows:

$$D_{i+1} = D_i + DDR_{i,s} \times PP \quad (3)$$

where PP is the required prediction period in years. The application of this equation seems straightforward but relying on two surveys to estimate the DDR may not reflect the actual deterioration; also,

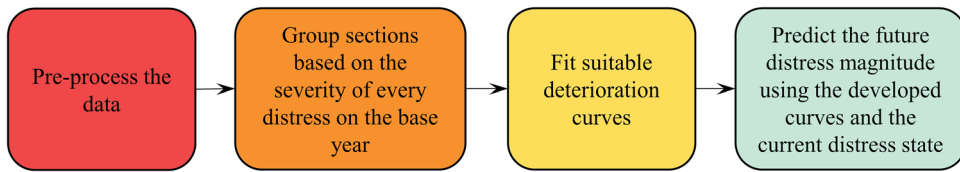


Figure 3. Flow chart explaining the methodology of the study.

it will not reflect the variability in the DDR from one section to another due to the variation of material properties for instance. Accordingly, it is suggested in this study to determine the DDR of a distress as an average of more than two previous measurements, which then can be utilised in predicting the future magnitude of that distress using the last survey results and the required prediction period by applying Equation (3). Figure 3 presents a flowchart explaining the developed methodology and how it can be implemented to determine DDRs and utilise these in predicting future distress levels. It must be stated here that the deterioration curves might be linear or nonlinear. This depends on the way the individual DDRs collapse onto each other to form a master curve; if the trend of the master curve is linear then a linear model should be fitted; if the trend is not linear then a suitable model should be fitted based on expert judgment.

3. Results and discussion

3.1. Distress deterioration rates

Following the methodology explained in the previous section the average DDRs of the three selected distress types, rutting in the left and right wheel paths, crack intensity over the whole carriageway, and texture depth, were determined as shown in Figures 4–7. Figure 4 and Figure 5 show the DDRs of rutting in the left and right wheel paths respectively. Interestingly, these figures show an approximately linear relationship between the average rutting of the sections of every group. They also show that the deterioration rate, which is expressed by the slope of the fitted lines, increases slightly with the increase of rutting severity. This can be explained by the fact that severe distress reduces the structural capacity of pavements, which leads to larger strain levels and eventually larger distress. It must be mentioned here that the rutting in the left wheel path did not correlate well with the rutting in the right wheel path, with a coefficient of correlation (R^2) less than 0.2. This can probably be explained by factors affecting rutting on roads such as effects of the cross slope on the distribution of traffic loading on the pavement, and on drainage where the lower side of a lane may become more saturated and eventually weaker than the higher side. Accordingly, two rutting models for the two wheel paths have been developed in this study as explained in later sections.

Figure 6 shows the deterioration trends of crack intensity over time. This figure demonstrates that cracking does not increase linearly but tends to take an exponential form. This means that cracking DDRs can be more progressive than other distress types such as rutting especially at high crack severities. The reasons behind this can be factors such as ageing which reduces strain tolerance of asphalt, pavement water damage once cracks are initiated, or general deterioration in the structural capacity of a pavement over its service life.

Lastly, Figure 7 presents the deterioration trends for texture depth; it can be seen that texture depth generally decreases over time. This is a normal trend for texture depth as it decreases due to abrasion of the pavement surface caused by vehicle tyres (Athiappan et al., 2022). The decrease rate, however, is dependent on the texture depth; the figure shows that sections with large initial texture exhibit faster reduction in texture depth than those with low texture. This is mostly like due to the larger the texture depth the bigger the frictional forces with vehicle tyres.

The above analysis is based on average DDRs. The variability amongst deterioration rates, however, could be large. This could be due to several factors including variability in traffic loading, pavement

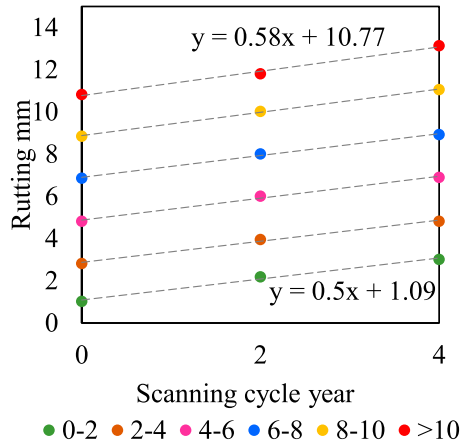


Figure 4. DDRs for rutting in the left wheel path.

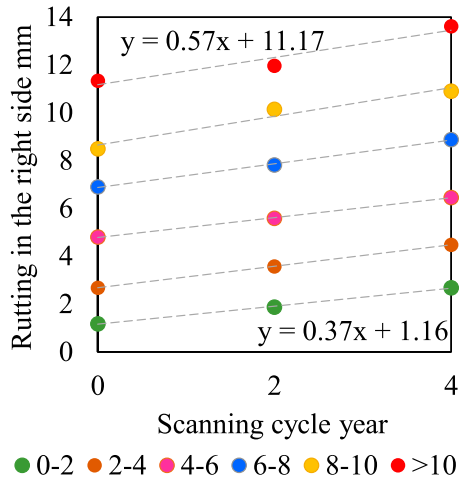


Figure 5. DDRs for rutting in the right wheel path.

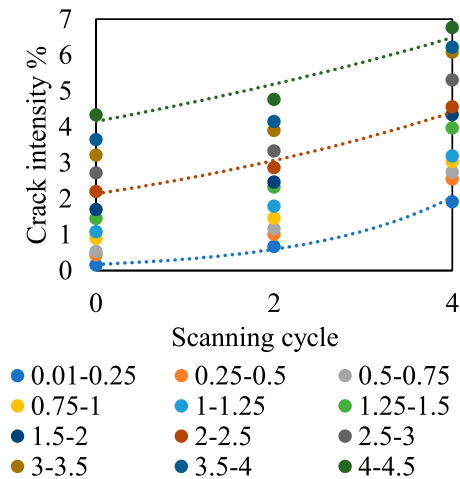


Figure 6. DDRs of the crack intensity over the whole carriageway.

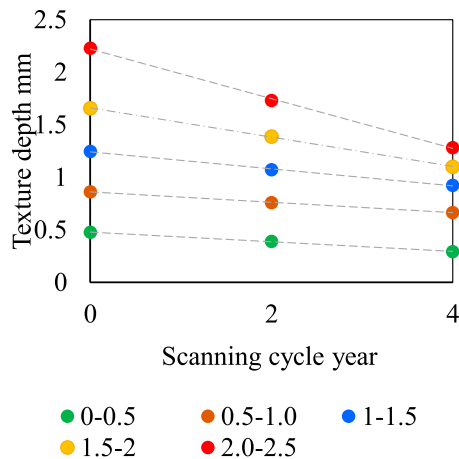


Figure 7. DDRs of the texture depth in the case of increasing texture over time.

structure, properties of pavement layers, environmental conditions, or even pavement geometry such as longitudinal and transverse profiles. The work presented in reference (Kargah-Ostadi et al., 2019) is based on the average deterioration in the PCI. The data collected in this study, however, shows that there is a large variability in deterioration rates. For instance, Table 3 indicates that the level of rutting variation in both wheel paths is from 6.7% to 61.3%. This means there is significant variability in the DDRs, and therefore this should be considered in the prediction process. To achieve that, three DDRs were developed for every distress type; the first represents the average deterioration, the second fits the 10th percentile of each severity group, the third represents the 90th percentile. The 10th and 90th percentiles were calculated by fitting a lognormal distribution and determining the distress values that match these reliability levels. Accordingly, three deterioration models are developed for every distress type, one at the average deterioration rate, one below the average which can be considered an optimistic prediction, and one above the average which accounts for a high level of deterioration around the worst-case scenario.

3.2. Distress deterioration master curves

The deterioration curves shown above can be applied directly to predict the future level of a particular distress type using Equation 3. Basically, one can use a suitable deterioration rate based on the current level of distress and the required prediction period. This means however that several deterioration curves should be used in the prediction process. Although this is achievable, a new method has been developed in this study to generate a single Distress Deterioration Master Curve (DDMC) that can be used in the prediction process.

By analysing the results in Figures 4–7 it can be seen that the distress results of individual groups can be collapsed onto one master curve. This can be achieved by shifting the x axis data to the right until all data form a smooth curve. The concept behind this idea is that the models of the individual groups can be represented by a single master model in which the slope of the master model matches the slopes of the individual models. In this case the deterioration rate of the individual groups, which is the slope of the individual lines, will match the deterioration rate of the fitted master curve. Caution should be taken when constructing master curves of this type as data shifting should be performed without changing the slope of the data. This has been accomplished by manually shifting the survey data to the right relative to the first group (lowest distress level) until a smooth curve is achieved. For example, the 2–4 mm group in Figure 4 was shifted to the right until this dataset formed a smooth line with the 0–2 mm group; all other groups were similarly shifted to the right until all of the groups formed

Table 3. Rutting data in the left and right wheel paths collected between 2014 and 2018.

Severity	Distress Year	Rutting in the right side			Rutting in the left side		
		2014	2016	2018	2014	2016	2018
0–2 mm	Mean	1.03	2.20	3.02	1.18	1.87	2.68
	Std	0.58	1.35	1.76	0.59	0.85	1.19
	CoV %	56.2	61.3	58.1	49.8	45.3	44.3
	10%	0.29	0.47	0.77	1.94	2.96	4.21
	90%	1.78	3.92	5.27	0.43	0.79	1.16
2–4 mm	Mean	2.83	3.96	4.83	2.69	3.57	4.49
	Std	0.58	1.28	1.59	0.54	1.11	1.39
	CoV %	20.4	32.4	32.9	20.0	31.1	31.0
	10%	2.09	2.32	2.80	3.38	4.99	6.27
	90%	3.57	5.61	6.86	2.00	2.15	2.70
4–6 mm	Mean	4.83	6.01	6.91	4.80	5.58	6.46
	Std	0.61	1.23	1.51	0.63	0.92	1.24
	CoV %	12.6	20.5	21.9	13.1	16.5	19.2
	10%	4.05	4.43	4.97	5.61	6.77	8.05
	90%	5.61	7.59	8.85	3.99	4.40	4.87
6–8 mm	Mean	6.86	8.02	8.93	6.90	7.82	8.88
	Std	0.61	1.21	1.48	0.69	0.97	1.79
	CoV %	8.9	15.1	16.5	10.0	12.4	20.2
	10%	6.08	6.47	7.04	7.79	9.06	11.18
	90%	7.64	9.57	10.82	6.01	6.58	6.59
8–10 mm	Mean	8.86	10.04	11.06	8.50	10.15	10.90
	Std	0.63	1.02	1.25	0.57	1.92	2.05
	CoV %	7.1	10.2	11.3	6.7	18.9	18.8
	10%	9.66	11.34	12.66	9.22	12.61	13.53
	90%	8.05	8.73	9.46	7.78	7.69	8.27
> 10 mm	Mean	10.83	11.82	13.14	11.34	11.97	13.62
	Std	0.88	0.92	1.28	1.90	1.75	1.70
	CoV %	8.1	7.8	9.8	16.8	14.6	12.5
	10%	9.71	10.63	11.50	13.78	14.21	15.80
	90%	11.96	13.00	14.78	8.90	9.72	11.44

a smooth line. It must be stated here that when shifting a data group to the right, the whole group is shifted to the right while maintaining a time difference of two years between the data points of that group, as the frequency of the surveys is one every two years. The y axis data on the other hand is kept the same when shifting the data, as shown in Figures 8–11. The exact same procedure is followed when constructing DDMCs at any selected reliability level. For example, to construct a deterioration master curve at 90% reliability level 90th percentiles of the data are used rather than averages, and these are grouped based on severity. The data of every severity group are then shifted to the right until a smooth curve is obtained as explained above, and lastly a suitable DDMC is fitted.

Figure 8 and Figure 9 show the DDMCs for rutting in the two-wheel paths. These figures show the average deterioration rates as well as the 10th and 90th percentiles. The main point to observe here is the closeness between the individual data sets and the master curves. If these two match each other, then the master curve will give good results. It must be mentioned here that despite Figure 4 and Figure 5 showing that rutting DDRs may increase over time, the largest increase is about 0.08 mm/year for rutting in the left wheel path and 0.2 mm/year for rutting in the right wheel path. Accordingly, linear models were fitted to the shifted data to model rutting deterioration behaviour, as shown in Figure 8 and Figure 9. Based on these figures, the DDRs in the left wheel path are 0.19, 0.52, and 0.95 mm at 10%, average and 90% reliabilities respectively, and 0.21, 0.46, and 0.79 mm in the right wheel path.

Following the same approach, DDMCs of crack intensity have been developed, as shown in Figure 10. In this figure, exponential models of the form $(a \times \exp(b \times x) - c)$ have been found to best fit the cracking data, with a coefficient of regression (R^2) greater than 0.95. This means that the deterioration rate for crack intensity is not linear but exponential related to the current intensity of the cracks. Lastly, Figure 11 presents the texture depth DDMCs, which shows that an exponential model provides

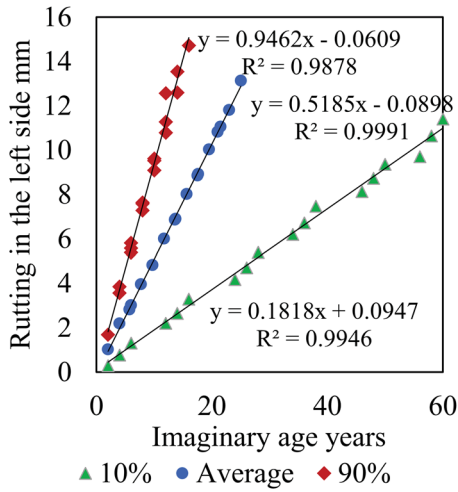


Figure 8. Deterioration curve for rutting in the left wheel path.

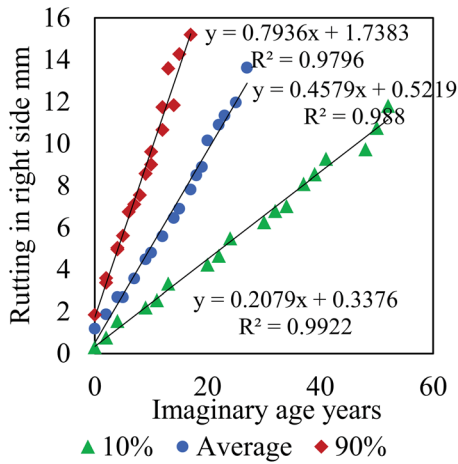


Figure 9. Deterioration curve for rutting in the right wheel path.

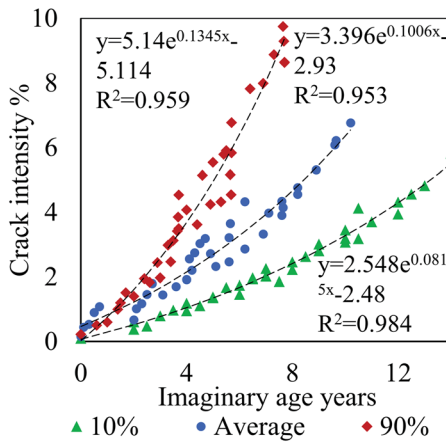


Figure 10. Deterioration curve for cracking over the whole carriageway.

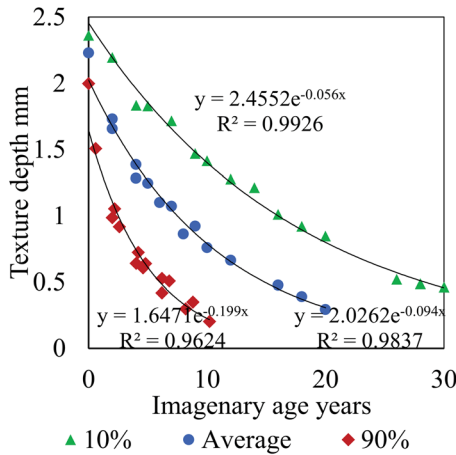


Figure 11. Deterioration curve for texture depth.

a very good fit with an R^2 of 0.98, except at 90% where the R^2 drops to 0.888, which still acceptably good. It must be stated here that the x-axis of the figures represents an ‘imaginary’ time with no absolute meaning; distress rate should be calculated based on the current distress level by inverting the deterioration models, as explained below.

The master curves can now be applied to predict the future level of distress by using the current distress measurements. With respect to rutting prediction on both wheel paths, Equation 3 can be applied directly using rutting DDRs at the selected reliability levels. With respect to crack intensity and texture depth the prediction process is less straightforward, because the deterioration rate is dependent on the level of distress. This can be calculated from the deterioration curves as follows:

- (1) Fit a curve to best match the behaviour of the data on the master curve; for the average crack intensity, the model below has been fitted:

$$Cl_i = 3.396 \times \exp(0.1006 \times T_i) - 2.93 \tag{4}$$

where Cl_i is the crack intensity at the current state.

- (2) By inverting Equation (4), the imaginary time associated with the current distress state can be calculated using the current distress measurement, as shown below:

$$T_i = \ln(5 \times (100 \times Cl_i + 293)/1698)/0.1006 \tag{5}$$

- (3) By adding the required prediction period to the results of Equation (5) and substituting the outcome to Equation (4), we obtain the following equation:

$$Cl_{i+1} = 3.396 \times \exp \left(0.1006 \times \left[\ln \left(5 \times \frac{100 \times Cl_i}{1698} \right) / 0.1006 + PP \right] \right) - 2.93 \tag{6}$$

Following the above steps, the crack intensity deterioration model at 10% and 90%, as well as the texture depth deterioration models at 10%, average, and 90% have been derived as shown in Table 4. The following section discusses the implementation of the developed deterioration curves in predicting pavement performance and any limitations associated with this method.

3.3. Distress prediction results

To demonstrate the application of the developed DDMCs and analyse their predictive accuracy, rutting in both wheel paths, crack intensity, and texture depth in 2020 were predicted based on the data

Table 4. Crack intensity and texture depth deterioration models at 10%, average, 90% reliability levels.

$CI_{i+1} = 2.548 \times \exp\left(0.0815 \times \left[\ln\left(10 \times \frac{25 \times CI_i + 62}{637}\right) / 0.0815 + PP\right]\right) - 2.48$	10%	Equation 7
$CI_{i+1} = 3.396 \times \exp\left(0.1006 \times \left[\ln\left(5 \times \frac{100 \times CI_i}{1698}\right) / 0.1006 + PP\right]\right) - 2.93$	Average	Equation 8
$CI_{i+1} = 5.14 \times \exp\left(0.1345 \times \left[\ln\left(\frac{500 \times CI_i + 2557}{2570}\right) / 0.1345 + PP\right]\right) - 5.114$	90%	Equation 9
$TD^*_{i+1} = 2.4552 \times e^{-0.056 \times (-\ln(TD_i / 2.4552) / 0.056 + PP)}$	10%	Equation 10
$TD_{i+1} = 2.0262 \times e^{-0.094 \times (-\ln(TD_i / 2.0262) / 0.094 + PP)}$	Average	Equation 11
$TD_{i+1} = 1.6471 \times e^{-0.199 \times (-\ln(TD_i / 1.64711) / 0.199 + PP)}$	90%	Equation 12

*TD stands for texture depth

collected in 2018. With respect to rutting prediction Equation (3) was applied directly by using the deterioration rates shown in Figure 8 and Figure 9, whereas for crack intensity and texture depth, Equations (7–12) were used. The prediction results are presented in Figure 12. This figure presents the measured distress from SCANNER in 2020 compared with the predicted distress using the deterioration models. It must be stated here that the 2018 SCANNER data was pre-processed using the outlier removal method to remove the sections that were maintained between 2018 and 2020, and also to remove sections that exhibited extreme deterioration, which may have been due to localised issues on the roads (Kargah-Ostadi et al., 2019). In this study, any deterioration more than two standard deviations above the mean was considered an outlier and excluded in the validation process. In practical applications of this work, pavement managers should have a record of any maintenance works that have taken place and any localised issues on their road network that can cause excessive deterioration in certain sections. These data will allow managers to remove these sections in the prediction process, and this will allow for a better implementation of the models.

Following these rules, the DDMCs were applied to predict the distress in 2020 at the selected reliability levels. Figure 12 A to F show rutting prediction results in both wheel paths at the selected reliability levels. The results in subfigure A were calculated by applying a deterioration rate of 0.1818 mm/year (as shown in Figure 8) in Equation (3), whereas a deterioration rate of 0.5158 mm/year was used in subfigure B, and a deterioration rate of 0.9462 mm/year was used in subfigure C. The deterioration rates applied in subfigures D, E and F are shown in Figure 9. Generally, these figures indicate that the larger the reliability level, the more the data shifted above the equality line. This is explained by the fact that at the 10th percentile, the deterioration rate will be below the average, which means the models will underestimate distress deterioration, whereas at the 90th percentile, the deterioration rate will be above the average, which means the models will overestimate the deterioration rates. Similar trends can be seen for crack intensity in Figure 12 G to I, and for the texture depth in Figure 12 J to L. The difference between rutting prediction and crack intensity/texture depth prediction is that the deterioration rate in rutting is constant at a given reliability level, whereas it is variable and dependent on the current distress state in the case of crack intensity and texture depth. Furthermore, to assess the statistical significance of the results, the Root Mean Square Error (RMSE) and R² were calculated, as shown in Table 5, which also presents the number of road sections used in the validation process. It can be seen that there is a generally good correlation between the measured and predicted data.

To further understand the accuracy of the predictions, it is necessary to set up some measures that can describe the accuracy in a more informative way. R² and RMSE are statistical measures that show how aligned and close the predictions are to the actual measurements in a macro sense. But to understand more about the accuracy of the predictions and analyse to what extent the models performed in an acceptable or unacceptable way, it is necessary to consider further measures that can give a deeper sense of the data. To achieve that, four descriptive measures have been considered in this study, these

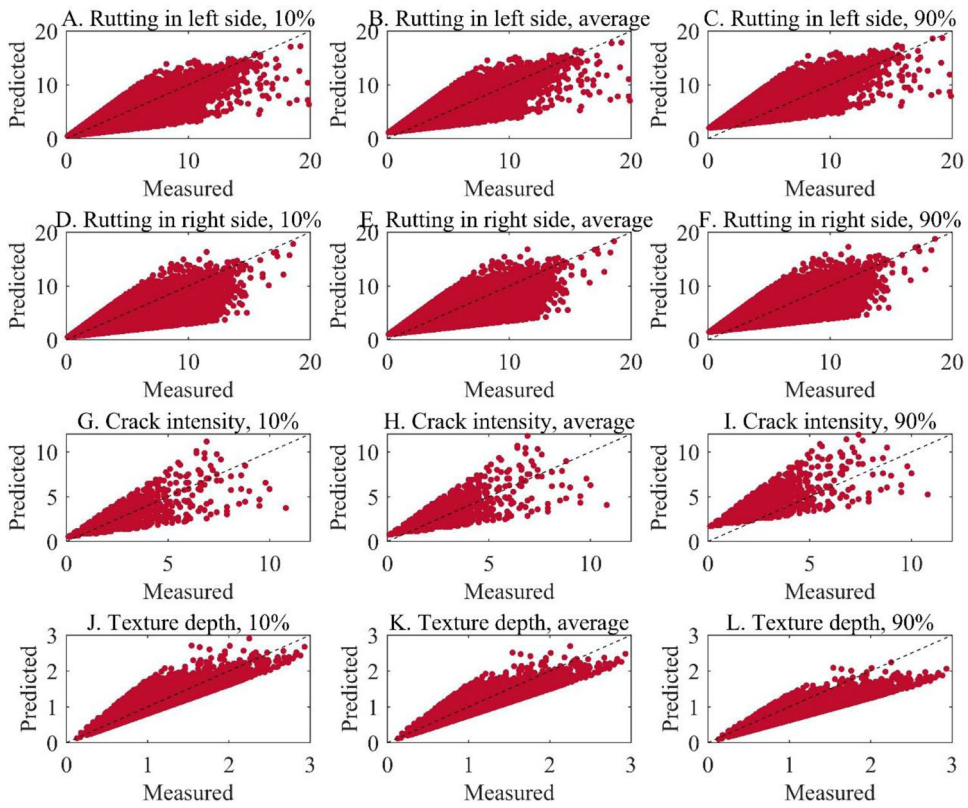


Figure 12. Distress predictions for year 2020 based on data collected in year 2018

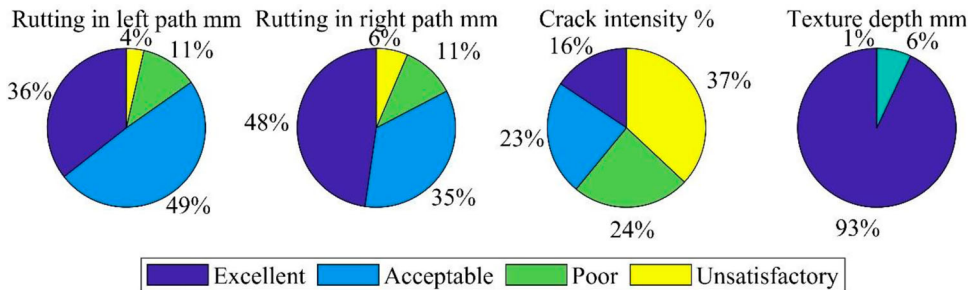
Table 5. Number of sections used in the validation process with, MSE, and R2 results.

Distress	Number of validation sections	RMSE at the average prediction	R ²
Rutting in left wheel path	28205	1.27	0.856
Rutting in right wheel path	34092	1.72	0.815
Crack intensity	2549	0.88	0.83
Texture depth	21931	0.15	0.916

are Excellent, Good, Poor, and Unsatisfactory. Every category of these measures has a predetermined absolute error; if the absolute error in the prediction data is smaller than the predetermined error, then that data set will be assigned to that specified category. In this case the results will be expressed as the percentages of the data matching the selected descriptive measures. The only issue with this approach is the values of the predetermined absolute errors. These error thresholds can significantly affect the interpretation of the results; therefore, they should be selected carefully. If they are too tight, then the results will be entirely unacceptable and vice versa; and unfortunately, no thresholds have been reported in the literature. Accordingly, the thresholds shown in Table 6 were selected based on expert judgement after careful consideration. Rutting prediction with an error up to 1 mm or crack intensity prediction with an error up to 0.25% or texture depth prediction with an error up to 0.15 mm are considered excellent predictions. Rutting prediction with an error more than 3 mm, crack intensity prediction with an error more than 0.75% or texture depth prediction with an error more than 1 mm are considered unsatisfactory predictions. Acceptable and poor prediction thresholds are between these extremes.

Table 6. Criteria considered to rank the accuracy of the distress predictions.

Distress	Excellent	Good	Poor	Unsatisfactory
Rutting mm	± 1.0	± 2.0	± 3.0	$> \pm 3.0$
Crack intensity %	± 0.25	± 0.5	± 0.75	$> \pm 0.75$
Texture depth mm	± 0.35	± 0.7	± 1.0	$> \pm 1.0$

**Figure 13.** Pie chart illustrating the ranking of the predicted distress accuracy.

Following this approach, the micro accuracy of the predictions, which is here defined as the accuracy of the individual predictions rather than the model as a whole, was analysed, as shown in Figure 13; this figure presents the percentages of the road sections that fall under the four descriptive measures. With respect to rutting, in general about 85–83% of the predictions fall under excellent to good predictions in both wheel paths. The texture depth showed the best prediction accuracy with 93% falling under excellent. Crack intensity, however, shows that 61% of the predictions fall in the poor or unsatisfactory categories. This is most likely due to the quality of the distress measurement data which has been reported as the most difficult one to quantify due to the similarity between this distress and other features on the road surface such as patches, fretting, ironwork, and high friction surfaces (McRobbie & Wright, 2006), which makes the quality of the crack intensity data less than the quality of other distress types.

4. Conclusions

In this study, an innovative practical method to model pavement deterioration using SCANNER data has been developed. This method utilises previous distress measurement data to estimate distress deterioration rates (DDRs) as a function of distress severity and use these to predict pavement performance. DDRs were determined by analysing SCANNER measurement data and grouping the distress into different levels based on their severity, modelling each group individually, combining the developed individual models into one deterioration model. To demonstrate the application of this method, a significant amount of SCANNER data for A roads in Nottinghamshire were employed in this study. The data were used to determine the DDRs of three main distress types: rutting, cracking, and texture depth. The DDRs were then used to predict distress in 2020 based on data collected in 2018. Based on the results of this study, the following conclusions can be drawn:

1. The developed method requires previous distress measurements to predict future condition; no data about pavement type, age or material properties are required, which makes it practical and easy to implement. But the prediction accuracy of this method relies significantly on the quality of the collected data.
2. The distress prediction results showed different levels of accuracy from excellent to unsatisfactory. This can probably be explained by factors such as: variability of pavement response from one

place to another, variability of pavement properties, effects of pavement maintenance on distress measurements, the accuracy of distress quantification and the uncertainty of the overall process.

3. Unlike Markov Chain methods, this method can be used to model pavement performance at both network level and project level, and it can be used to predict the performance of individual sections and locate those requiring maintenance or further investigation.
4. Three distress predictions have been modelled in this study, at 10th percentile, average, and 90th percentile deterioration rates. The first is an optimistic prediction, the second is realistic and may produce the lowest error in the prediction process, the last may overestimate the deterioration rate, but this may be desirable when making pavement management and maintenance plans, to be on the safe side.
5. Although this method was developed based on A roads in Nottinghamshire, UK, the methodology to extract distress deterioration curves is valid for all road classes and for all distress types. This means that a tailored set of deterioration curves can be developed for every authority reflecting the environmental conditions of their region, material properties, their pavement structures and traffic volumes.

The current work has been conducted based on a static prediction of distress deterioration; thus, a certain deterministic deterioration is assigned to the current distress state to predict the future. Future work will focus on developing a dynamic deterioration prediction model, in which the deterioration rate will not be a constant value but a dynamic one estimated based on the distress deterioration probability distribution function and past SCANNER data.

Acknowledgement

The authors would like to acknowledge Neil Butler, Peter Wells, and Ian Patchett from Via East Midlands for providing the data and for their technical support during the development of this work.

Disclosure statement

No potential conflict of interest was reported by the author(s).

Funding

This work was supported by the Engineering and Physical Sciences Research Council [grant number EP/T01962X/1].

Data availability

The data underlying this article will be made available upon reasonable request from the corresponding author subject to data owner approval.

ORCID

Ahmed Abed  <http://orcid.org/0000-0002-6822-5519>

References

- Abaza, K. A. (2014). Back-calculation of transition probabilities for Markovian-based pavement performance prediction models. *International Journal of Pavement Engineering*, 17(3), 253–264. <https://doi.org/10.1080/10298436.2014.993185>
- Abaza, K. A. (2015). Simplified staged-homogenous Markov model for flexible pavement performance prediction. *Road Materials and Pavement Design*, 17(2), 365–381. <https://doi.org/10.1080/14680629.2015.1083464>
- Abed, A., Thom, N., & Neves, L. (2019). Probabilistic prediction of asphalt pavement performance. *Road Materials and Pavement Design*, 20(sup1), S247–S264. <https://doi.org/10.1080/14680629.2019.1593229>
- Abu Al-Rub, R. K., Darabi, M. K., Huang, C.-W., Masad, E. A., & Little, D. N. (2012). Comparing finite element and constitutive modelling techniques for predicting rutting of asphalt pavements. *International Journal of Pavement Engineering*, 13(4), 322–338. <https://doi.org/10.1080/10298436.2011.566613>

- Ahlin, K., & Granlund, N. O. J. (2011). Relating road roughness and vehicle speeds to human whole body vibration and exposure limits. *International Journal of Pavement Engineering*, 3(4), 207–216. <https://doi.org/10.1080/10298430210001701>
- Alavi, M., Hajj, E. Y., & Sebaaly, P. E. (2015). A comprehensive model for predicting thermal cracking events in asphalt pavements. *International Journal of Pavement Engineering*, 18(9), 871–885. <https://doi.org/10.1080/10298436.2015.1066010>
- Alimoradi, S., Golroo, A., & Asgharzadeh, S. M. (2020). Development of pavement roughness master curves using Markov Chain. *International Journal of Pavement Engineering*, 23(2), 453–463. <https://doi.org/10.1080/10298436.2020.1752917>
- ARA. (2004). *Guide for Mechanistic-Empirical Design of New and Rehabilitated Pavement Structures*. Asphalt Industry Alaiance. (2022). *Annual Local Authority Road Maintenance Survey*.
- Athiappan, K., Kandasamy, A., Mohamed, M. J. S., Parthiban, P., & Balasubramanian, S. (2022). Prediction modeling of skid resistance and texture depth on flexible pavement for urban roads. *Materials Today: Proceedings*, 52, 923–929. <https://doi.org/10.1016/j.matpr.2021.10.304>
- Chan, C. Y., Huang, B., Yan, X., & Richards, S. (2010). Investigating effects of asphalt pavement conditions on traffic accidents in Tennessee based on the pavement management system (PMS). *Journal of Advanced Transportation*, 44(3), 150–161. <https://doi.org/10.1002/atr.129>
- Chu, C., Wang, L., & Xiong, H. (2022). A review on pavement distress and structural defects detection and quantification technologies using imaging approaches. *Journal of Traffic and Transportation Engineering (English Edition)*, 9(2), 135–150. <https://doi.org/10.1016/j.jtte.2021.04.007>
- Darter, M. I., & Hudson, W. R. (1973). Probabilistic design concepts applied to flexible pavement system design.
- Dave, E. V., & Buttlar, W. G. (2010). Thermal reflective cracking of asphalt concrete overlays. *International Journal of Pavement Engineering*, 11(6), 477–488. <https://doi.org/10.1080/10298430903578911>
- Department for Transport. (2012). *Guidance on road classification and the primary route network*. Department for Transport. Retrieved February 23, from <https://www.gov.uk/government/publications/guidance-on-road-classification-and-the-primary-route-network/guidance-on-road-classification-and-the-primary-route-network>
- Department for Transport. (2021). *Technical Note: Road condition and maintenance data*.
- Di Benedetto, H., De La Roche, C., Baaj, H., Pronk, A., & Lundström, R. (2004). Fatigue of Bituminous Mixtures. RILEM TC 182-PEB 'Performance testing and evaluation of bituminous materials.
- Dinegdae, Y. H., & Birgisson, B. (2016). Effects of truck traffic on top-down fatigue cracking performance of flexible pavements using a new mechanics-based analysis framework. *Road Materials and Pavement Design*, 19(1), 182–200. <https://doi.org/10.1080/14680629.2016.1251958>
- Epps, A. (2000). Design and analysis system for thermal cracking in Asphalt Concrete. *Journal of Transportation Engineering*, 126(4), 300–307. [https://doi.org/10.1061/\(ASCE\)0733-947X\(2000\)126:4\(300\)](https://doi.org/10.1061/(ASCE)0733-947X(2000)126:4(300))
- Guha, S., & Hossain, K. (2022). An economic approach to road condition assessment using road user feedback: A new model and its application. *International Journal of Pavement Engineering*, 1–16. <https://doi.org/10.1080/10298436.2021.2022673>
- Kargah-Ostadi, N., & Stoffels, S. M. (2015). Framework for development and comprehensive comparison of empirical pavement performance models. *Journal of Transportation Engineering*, 141(8), [https://doi.org/10.1061/\(ASCE\)TE.1943-5436.0000779](https://doi.org/10.1061/(ASCE)TE.1943-5436.0000779)
- Kargah-Ostadi, N., Zhou, Y., & Rahman, T. (2019). Developing performance prediction models for pavement management systems in local governments in absence of age data. *Transportation Research Record: Journal of the Transportation Research Board*, 2673(3), 334–341. <https://doi.org/10.1177/0361198119833680>
- Kim, H. B., Buch, N., & Park, D.-Y. (2000). Mechanistic-Empirical rut prediction model for In-service pavements. *Transportation Research Record*, 1730(1), 99–109. <https://doi.org/10.3141/1730-12>
- Luo, X., Gu, F., Ling, M., & Lytton, R. L. (2018). Review of mechanistic-empirical modeling of top-down cracking in asphalt pavements. *Construction and Building Materials*, 191, 1053–1070. <https://doi.org/10.1016/j.conbuildmat.2018.10.005>
- Luo, X., Gu, F., Zhang, Y., Lytton, R. L., & Zollinger, D. (2017). Mechanistic-empirical models for better consideration of subgrade and unbound layers influence on pavement performance. *Transportation Geotechnics*, 13, 52–68. <https://doi.org/10.1016/j.tgeo.2017.06.002>
- Mansura, D. A., Thom, N. H., & Beckedahl, H. J. (2018). Numerical and experimental predictions of texture-related influences on rolling resistance. *Transportation Research Record: Journal of the Transportation Research Board*, 2672(40), 430–439. <https://doi.org/10.1177/0361198118776114>
- Marcelino, P., de Lurdes Antunes, M., Fortunato, E., & Gomes, M. C. (2019). Machine learning approach for pavement performance prediction. *International Journal of Pavement Engineering*, 22(3), 341–354. <https://doi.org/10.1080/10298436.2019.1609673>
- Mbarki, R., Kutay, M. E., Gibson, N., & Abbas, A. R. (2012). Comparison between fatigue performance of horizontal cores from different asphalt pavement depths and laboratory specimens. *Road Materials and Pavement Design*, 13(3), 422–432. <https://doi.org/10.1080/14680629.2012.685843>
- McRobbie, S., Walter, L., Read, C., Viner, H., & Wright, A. (2007). Developing SCANNER road condition indicator parameter thresholds and weightings-version 1. *TRL Published Project Report*.
- McRobbie, S., & Wright, A. (2006). *TTS Research-Crack detection on local roads. Phase 1*.
- Můčka, P. (2016). International Roughness Index specifications around the world. *Road Materials and Pavement Design*, 18(4), 929–965. <https://doi.org/10.1080/14680629.2016.1197144>

- Perraton, D., Di Benedetto, H., Sauzéat, C., De La Roche, C., Bankowski, W., Partl, M., & Grenfell, J. (2010). Rutting of bituminous mixtures: Wheel tracking tests campaign analysis. *Materials and Structures*, 44(5), 969–986. <https://doi.org/10.1617/s11527-010-9680-y>
- Perrotta, F., Parry, T., Neves, L. C., Buckland, T., Benbow, E., & Mesgarpour, M. (2019). Verification of the HDM-4 fuel consumption model using a Big data approach: A UK case study. *Transportation Research Part D: Transport and Environment*, 67, 109–118. <https://doi.org/10.1016/j.trd.2018.11.001>
- PTS. (2022). *Surface Condition Assessment for the National Network of Roads*. Pavement Testing Services. Retrieved April 27, from <http://www.ptsinternational.co.uk/scanner-2/>
- Ragnoli, A., De Blasiis, M., & Di Benedetto, A. (2018). Pavement distress detection methods: A review. *Infrastructures*, 3(4), 58–77. <https://doi.org/10.3390/infrastructures3040058>
- Sandra, A. K., & Sarkar, A. K. (2013). Development of a model for estimating international roughness index from pavement distresses. *International Journal of Pavement Engineering*, 14(8), 715–724. <https://doi.org/10.1080/10298436.2012.703322>
- Shtayat, A., Moridpour, S., Best, B., Shroff, A., & Raol, D. (2020). A review of monitoring systems of pavement condition in paved and unpaved roads. *Journal of Traffic and Transportation Engineering (English Edition)*, 7(5), 629–638. <https://doi.org/10.1016/j.jtte.2020.03.004>
- Svenson, G., & Fjeld, D. (2015). The impact of road geometry and surface roughness on fuel consumption of logging trucks. *Scandinavian Journal of Forest Research*, 31(5), 526–536. <https://doi.org/10.1080/02827581.2015.1092574>
- Tamakloe, R., Lim, S., Sam, E. F., Park, S. H., & Park, D. (2021). Investigating factors affecting bus/minibus accident severity in a developing country for different subgroup datasets characterised by time, pavement, and light conditions. *Accident Analysis & Prevention*, 159, 106268. <https://doi.org/10.1016/j.aap.2021.106268>
- UK Roads Board. (2011a). *SCANNER surveys for Local Roads - User Guide and Specification - Advice to Local Authorities: Using SCANNER survey results*.
- UK Roads Board. (2011b). *SCANNER surveys for Local Roads - User Guide and Specification - Introduction to SCANNER surveys*.
- Wang, C., Xu, S., Liu, J., Yang, J., & Liu, C. (2022). Building an improved artificial neural network model based on deeply optimizing the input variables to enhance rutting prediction. *Construction and Building Materials*, 348. <https://doi.org/10.1016/j.conbuildmat.2022.128658>
- Wang, F., Machemehl, R. B., & Popova, E. (2010). Toward Monte Carlo simulation-based mechanistic-empirical prediction of Asphalt pavement performance. *Journal of Transportation Engineering*, 136(7), 678–688. [https://doi.org/10.1061/\(ASCE\)0733-947X\(2010\)136:7\(678\)](https://doi.org/10.1061/(ASCE)0733-947X(2010)136:7(678))
- Xiao, S.-Q., Tan, T., Xing, C., & Tan, Y. (2020). A contribution to texture analysis of pavements under simulated polishing: Some new findings. *International Journal of Pavement Engineering*, 23(7), 2370–2379. <https://doi.org/10.1080/10298436.2020.1855351>
- Yu, J., Chou, E. Y. J., & Luo, Z. (2007). Development of linear mixed effects models for predicting individual pavement conditions. *Journal of Transportation Engineering*, 133(6), 347–354. [https://doi.org/10.1061/\(ASCE\)0733-947X\(2007\)133:6\(347\)](https://doi.org/10.1061/(ASCE)0733-947X(2007)133:6(347))
- Zhou, Q., Okte, E., & Al-Qadi, I. L. (2021). Predicting pavement roughness using Deep Learning algorithms. *Transportation Research Record: Journal of the Transportation Research Board*, 2675(11), 1062–1072. <https://doi.org/10.1177/03611981211023765>
- Ziari, H., Sobhani, J., Ayoubinejad, J., & Hartmann, T. (2015). Analysing the accuracy of pavement performance models in the short and long terms: GMDH and ANFIS methods. *Road Materials and Pavement Design*, 17(3), 619–637. <https://doi.org/10.1080/14680629.2015.1108218>